RICE UNIVERSITY

Simulation of Shielding Materials against Galactic Cosmic Rays
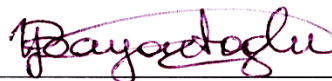
by

Xindi Li

A Thesis Submitted
in Partial Fulfillment of the
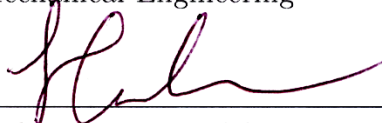Requirements for the Degree
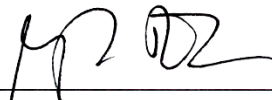
Master of Science

Approved, Thesis Committee:

Yildiz Bayazitoglu, Chair
H. S. Cameron Chair Professor of
Mechanical Engineering

Pedram Hassanzadeh
Assistant Professor of Mechanical
Engineering

Robert Vajtai
Senior Faculty Fellow of Materials Science
and Nanoengineering

Houston, Texas

April, 2017

This thesis is dedicated to my mom and dad, thank you for making me feel loved and supported every single day. And to my husband Chengchen, the best listener in the world and the loyalest friend of mine. To my adviser, professor Yildiz Bayazitoglu, who has been so inspiring to me as an extraordinary woman in everything. And to my colleagues and friends, I'm so grateful to have all of you by my side.

ABSTRACT

Simulation of Shielding Materials against Galactic Cosmic Rays

by

Xindi Li

Radiation is one of the most critical hazards for deep space missions. Among the sources of deep space radiation, the Galactic Cosmic Rays, which are composed of high energy ions travelling at relativistic speeds from outside the solar system, are especially difficult to shield. As spacefaring nations have progressed in their exploration activities, there has been increasing interest in longer and deeper space voyages. However, beyond Low Earth Orbit, without the protection afforded by the Earth's magnetic field, long space voyages have increased risks from radiation exposure. Hence more efficient shielding materials are necessary for solving this radiation issue.

Space radiation shielding can be examined by either ground-based experiments or simulations. Deterministic or Monte Carlo approaches are the two computational methods to simulate the radiation transport problem. MULASSIS, a Monte Carlo code developed by QinetiQ, BIRA and ESA is based on Geant4 and is used in this thesis.

A convergence study is first performed with aluminum as a shielding material in order to determine the number of primary particles to use in the MULASSIS simulations. Dose equivalent analysis is then performed for single shielding materials with updated radiation weighting factors recommended in ICRP 103, including aluminum,

polyethylene, boron nitride infused with hydrogen and liquid hydrogen. Dose equivalent depth curves are plotted for each shielding material, and in addition for various multilayer combinations of aluminum and the other materials. Because the biological impact from secondary produced neutrons can be so harmful, a fluence analysis is performed for various elemental components of the GCR radiation spectrum for different shielding materials.

Contents

Illustrations

Tables

Nomenclature

AU The astronomical unit is a unit of length, roughly the distance from Earth to the Sun

$BIRA$ Royal Belgian Institute for Space Aeronomy

$CERN$ the European Organization for Nuclear Research

$CREME$96 The Cosmic Ray Effects on Micro-Electronics (1996 Revision)

ESA The European Space Agency

GCR Galactic Cosmic Rays

$Geant$ The GEometry ANd Tracking toolkit

HZE High atomic number and energy particles

$ICRP$ The International Commission on Radiological Protection

ISS International Space Station

LEO Low Earth Orbit

$MULASSIS$ the Multi-Layered Shielding Simulation Software tool

$NCRP$ National Council on Radiation Protection and Measurements

SPE Solar Particle Events

$SPENVIS$ Space Environment, Effects, and Education System

Chapter 1

Introduction

1.1 Background

The hazardous radiation environment is one of the most critical issues to be addressed for space missions. Recently, there has been increasing interest in deep space missions beyond Low Earth Orbit (LEO). Within LEO, the Earth's magnetic field serves as a protection that deflects the low energy ions from space. However, beyond LEO, this protection no longer exists. Even worse, the exposure to space radiation accumulates over the long duration of missions into deeper space. Because of payload limitations, simply increasing the mass of shielding is not an option. Thus more effective shielding materials and configuration are currently the only practical solution to the problem.

1.2 Framing the problem

Primary sources of the radiation in deep space are the Solar Particle Events (SPEs) and the Galactic Cosmic Rays (GCR). The GCR is relatively much harder to shield than the SPEs.

GCR particles travel at near relativistic speeds from outside the solar system with energies ranging up to 10 GeV/nucleon, or more. The high energy GCR particles can penetrate the spacecraft and produce secondary particles in this process. The GCR ions and the secondaries interact with molecules in cells, alter DNA, and can cause severe damage to the human body. The National Council on Radiation Protection

and Measurements (the NCRP) has thus recommended the career dose limits for astronauts. Without improved shielding materials, there are severe limitations for space exploration into deeper space and for longer time periods.

Shielding from these radiation hazards has been a significant topic for decades. Passive shielding has been employed and improved for better effectiveness. Active shielding is a promising method, but is still under development. In terms of passive shielding, elements with the largest charge-to-mass ratio appear to be the best shielding material against HZE. [2] Currently, aluminum is the most widely used passive shielding material for spacecrafts. Though structurally stable, aluminum is not theoretically as good a shielding material as materials with higher hydrogen content. The recent advancement in material science and nanoengineering has shed some light on new potential shielding materials. Several materials have been proposed which provide good hydrogen storage, and thus may be good candidates for shielding against GCR.

Multilayered shielding is another possible solution to the radiation issue, with each layer addressing a unique characteristic of the incoming space radiation. For example, a combination of aluminum and polyethylene is used by NASA in the ISS. [3] This dual-layer structure has a much better shielding effectiveness than a single aluminum layer of the same areal densities (g/cm^2). [4]

Radiation transport codes have been widely used to study shielding materials. Available deterministic codes solve the 1D Boltzmann equations. Generally, a deterministic code runs very fast but its results are approximated in order to solve the integro-partial differential equations. On the other hand, Monte Carlo codes use stochastic methods to solve the Boltzmann equations in three dimensions. Therefore, Monte Carlo codes result in a more time consuming simulation. GEANT4 is

an open source Monte Carlo code developed by CERN written in C++. QinetiQ, BIRA and ESA have developed MULASSIS [5] (the Multi-Layered Shielding Simulation Software tool) based on GEANT4, which provides simplified geometry options but inherits most functions of Geant4.

Effective shielding materials can be the most practical solution to deep space GCR radiation issue. State-of-the-art materials and several multilayered configurations have been studied with the up-to-date MULASSIS simulation codes in this thesis in order to find possible candidates for more effective GCR shielding.

1.3   Approach

The simulation of radiation shielding problems involve the following steps: modeling the outer radiation environment, simulating the radiation transport process in the shielding material, and measuring the final impact of radiation on the target.

The simulation methods and software used in this thesis are introduced in chapter 2. The radiation environment, particularly Galactic Cosmic Radiation and its effect, as well as the physics of radiation transport are introduced in chapter 3.

Current and the state-of-the-art shielding strategies and shielding materials are discussed in chapter 4. Before the simulation of shielding materials, a convergence study is first performed to verify that the most appropriate number of primary particles has been used in MULASSIS. The simulation geometry is composed of semi-infinite slabs made of different shielding materials and a water phantom of 30 g/cm^2 to model the target— the human body.

To study GCR's biological impact on the human body, dose equivalent analysis is performed. The absorbed dose deposited into a water phantom for different materials of varying areal densities (g/cm^2) are collected and plotted. When comparing shield-

ing materials, a better material should result in more decrease in the dose equivalent at the same areal densities. Furthermore, results attained in this work used radiation weighting factors from the ICRP 103 [1], and have been compared with the results calculated with the preliminary ICRP 60 radiation weighting factors.

Besides the attenuation of the dose equivalent, a good shielding material should also produce less secondaries, including neutrons, when interacting with the GCR. To study this performance characteristic of shielding materials, the outbound flux of the biologically harmful secondary neutrons are collected at the boundary of the shielding material for different elemental components of the GCR. Since the biological damage caused by a neutron is highly dependent on its energy, the flux of secondary neutrons are plotted three dimensionally with varying energy and areal density.

Chapter 2

Radiation Transport Codes

Radiation shielding can be examined experimentally or through transport codes simulations. The Boltzmann Transport Equations are the governing equations for radiation transport problems and can be solved with either deterministic or Monte Carlo method.

2.1   Monte Carlo method

The Monte Carlo method is a statistical computation that can solve the Boltzmann equations numerically with the probability density functions (PDFs) for each step of the simulation. It allows particle transport in three dimensions in complex geometries. To obtain results with satisfying accuracy, Monte Carlo codes can be more time consuming to run than Deterministic codes. [6] Widely used Monte Carlo codes include Geant4, MULASSIS, FLUKA, PHITS, etc.

2.2   Deterministic method

Available deterministic methods solve the one dimensional integro-partial differential Boltzmann Transport Equations with a straight-ahead approximation. Running a deterministic code can be extremely fast, but systematic errors are inevitable. [6] Typical Deterministic codes include HZETRN developed by NASA Langley Research Center, and IPROP from the Naval Research Lab.

2.3 Geant4

Geant4 is a Monte Carlo tookit developed by CERN to simulate high energy particle interactions. It has been used widely in space science, medical applications, accelerator and nuclear physics. The code is implemented using Object Oriented Programming with C++. Geant4 covers comprehensive physics models, including electromagnetic, hadronic, transportation, decay, optical, photolepton_hadron, and parameterisation. [7] Electromagnetic model is the most important physics model for evaluating GCR shielding.

In Geant4, primary incident particles are tracked as they travel through the user-defined geometry, and its interaction with the matter is recorded. The result is then output in the form requested by user.

As a Monte Carlo code, Geant4 theoretically gives the finer results when more incident beams are used for calculation. However, this also means it can take very long run time to achieve statistical accuracy, highly depending on the performance of CPU. This situation is especially common when running heavier particles traversing thicker matter.

2.4 MULASSIS

The Multi-Layered Shielding Simulation Software (MULASSIS) was developed later, based on Geant4 by QinetiQ, BIRA and ESA. MULASSIS provides a user-friendly interface and can simulate the particle interactions with almost any shielding materials for both primary and secondary particles. [5] MULASSIS inherits most functions of Geant4 and is more user friendly thus requiring much less time before the user can start working with it.

MULASSIS allows slab or sphere geometry of up to 26 layers. In slab geometry, the incident beam is generated along the thickness. The beam can be only one type of particle at a time, which is different from HZETRN. But this allows its users to study the separate contribution to fluence and dose by different types of input particles. The energy spectrum and related flux ($MeV^{-1}cm^{-2}s^{-1}$) of each particle can be defined by the user. The angular distribution of a primary beam can be parallel, point source or omnidirectional. In this thesis, the energy spectrum data are inputted in tabulated mode based on the CREME96 output. The angular distribution of incident beams is defined as omnidirectional. Options for outputs of MULASSIS include fluence counted on the boundaries of a layer, total ionizing dose or total non-ionizing dose collected in a layer, and pulse height spectrum (PHS). Fluence in $particles/cm^2$ and total ionizing dose in Gy have been selected as output units in this thesis.

Chapter 3

Radiation Hazards in Deep Space

Deep space is defined as the space environment beyond the Earth radiation belts. For radiation protection study purposes, the space at 1 AU from the Sun and without a planetary magnetic field models deep space environment. [8] Below Low Earth Orbit (LEO), the Earth's magnetic field deflects most of the space radiation. Without this protection, deep space missions are faced directly with the threats from space radiation.

The primary sources of the radiation in deep space are the Solar Particle Events (SPEs) and the Galactic Cosmic Rays (GCR). The SPE is generated inside the solar system. It is composed mostly of protons, but it also includes helium nuclei and HZE. The SPE can carry energy up to a few 100 MeV/n, and due to their short duration are more easily predicted and avoided with current shielding strategies. [9]

Compared to SPE, GCR has generally a smaller flux, but is of much higher energy. The GCR particles travel at near relativistic speeds, i.e. speeds that are comparable to the speed of light, come from outside the solar system, and carry energies of 10 GeV/nucleon or more. [10] The GCR is composed of 85 percent protons, 14 percent α particles, and 1 percent higher atomic number ions. [9] Unlike most SPE particles which can be stopped by adequate shielding, GCR particles penetrate the spacecraft and other surfaces, and produce secondary particles, including neutrons, lighter nuclei, gamma rays and electrons. These secondaries carry the transferred high energy deeper into shielding materials. More detailed physics interactions are discussed in section

3.2 and 3.3. With all the features mentioned above, GCR particles are very hard to shield and are thus the focus of this thesis. The GCR particles at 1 AU from the Sun are applied as boundary conditions in the simulations.

3.1   Galactic Cosmic Rays (GCR)

Galactic Cosmic Rays are the highly energetic nuclei coming from outside the Solar System. Because of this distant origin and the scattering in their trajectories, the GCR particles can be considered fully ionized and isotropic. [8]

Although the flux of GCR is relatively small, its contribution to ionizing radiation and biological impact is crucial. The solar activity has a cycle of approximately 11 years. The intensity of GCR varies with solar activity. GCR intensity is at the maximum when the solar activity comes to its minimum, which is opposite to SPE. This is most likely because of the weakening of the interplanetary magnetic field during the weakening of solar activity, which allows more GCR particles travelling into the Solar System. [2]

Bernabeu et al. [8] considered GCR proton, helium and iron ions in their radiation shielding study. Protons are the predominated particle in the GCR fluence, helium nuclei take up 14 percent. Although heavier ions take up only around 1% of the total flux, they are much more damaging as they carry high energies and inevitably produce more secondaries. Therefore, apart from the two light nuclei, iron ion is also considered in this thesis for it's relatively high fluence as an HZE ion.

The GCR model used in this thesis is the CREME96 model [11] during the worst-case scenario 1977 Solar minimum. The model is accessible through SPENVIS and is processed and used as the input to MULASSIS in units of flux ($MeV^{-1}cm^{-2}s^{-1}$). CREME96 covers all ions from H to U, in unit of differential flux ($MeV^{-1}m^{-2}sr^{-1}s^{-1}$)
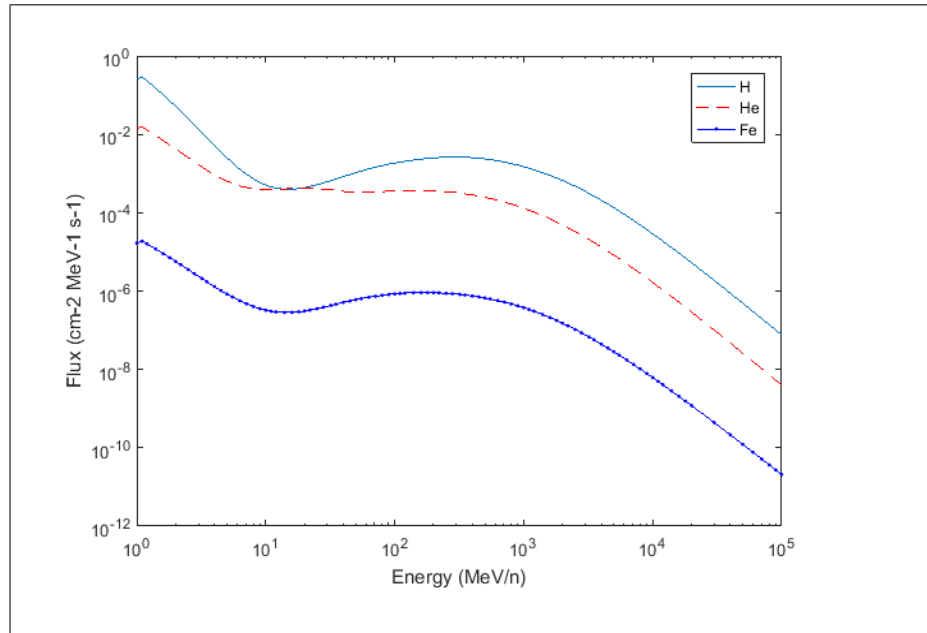
Figure 3.1 : CREME96 Galactic Cosmic Rays (GCR) Energy Spectrum during 1977 Solar Minimum for H, He, and Fe

and integrated flux $(m^{-2}s^{-1}sr^{-1})$. Figure 3.1 shows an energy spectrum of the CREME96 in units of differential flux $(MeV^{-1}cm^{-2}s^{-1})$ for hydrogen, helium and iron nuclei. Only fully ionized ions are considered in this thesis.

3.2   Ionizing radiation and its biological impact

When GCR ions penetrate a material, intense ionization takes place. Ionizing radiation is a radiation that carries sufficient energy to allow freeing of electrons from the atoms or molecules in the material. Ionizing radiation can be classified into direct ionizing radiation and indirect ionizing radiation. Accordingly, the most crucial interactions are electromagnetic interactions and nuclear interactions.

Direct ionizing radiation involves charged particles like protons, α particles, β

particles, and HZE ions. The Coulomb force is the dominant force in direct ionization. By electromagnetic inelastic collisions, these charged particles lose their kinetic energy primarily through excitation and ionization of the electrons in the target material. The loss of kinetic energy make them decelerated and eventually stopped.

Indirect ionizing radiation is the process by which particles with no charge lose their kinetic energy during nuclear interactions. Primary Galactic Cosmic Rays don't have uncharged particles, but during the interactions with shielding and the target, uncharged particles like neutrons and gamma rays are produced.

Neutron radiation is one of the most dangerous indirect ionizing radiations species. While high and medium energy neutrons are rather easy to stop, low energy neutrons experience complex hadronic interactions in the shielding material and are very hard to stop. [6] Neutrons can cause severe biological damage for this reason. Therefore, although secondary radiation is of overall lower energy and lower flux, it significantly increases the biological damage.

When cell DNAs are exposed to ionizing radiation, dislocation and breakage are caused by direct action, while reactive free radicals are formed by indirect action, which contributes 2/3 of the DNA damage. Damage can also be caused on the cell and tissue level. [12]

3.3   Energy loss and deposition

During the interactions between ionizing radiation and the target materials, the radiation loses energy and the energy transferred is deposited in the target. Two concepts have been introduced to measure the energy change.

Stopping power is defined as the average energy loss of a charged particle per unit distance in the target material, defined as $\Delta \mathrm{L} = -\frac{dE}{dx}$ (MeV/mm). Here, dE stands

for the energy loss of the radiation particles, while dx is the distance that the particles have traveled.

Linear Energy Transfer (LET) is used to quantify the energy locally deposited in the target material. The LET is defined as $\Delta L = \frac{dE}{dx}$ $(keV/\mu m)$. However in the LET, dE is the energy deposited into the target material, while dx is the distance that the particle has traveled.

Compared with stopping power, linear energy transfer does not consider the secondary radiation, which includes Bremsstrahlung, secondary protons and neutrons. In other words, the total stopping power includes the vital nuclear stopping power which is absent in LET. For this reason, though the two values can be very similar, LET is smaller than stopping power. [12]

Both stopping power and LET values depend on the properties of both projectile and target. In the Bethe-Bloch formula, which is an approximation to stopping power, the influencing factors include the projectile energy, charge, and speed, as well as a target's electron number density and mean excitation potential.

Generally, high LET stands for large energy transfer and therefore indicates good shielding effectiveness against ionizing radiation. This can be achieved with materials of high charge-to-mass ratio, which means that the material has a large number of loosely bound electrons per unit mass. [2] With more electrons, more electromagnetic inelastic collisions are likely to take place, i.e. more kinetic energy is lost through the ionization and excitation of the electrons. For example, hydrogen is proposed to be the most effective shielding material because it has the highest charge-to-mass ratio.

In order to better compare the shielding effectiveness of different shielding materials, the unit areal density g/cm^2, which is the product of density and depth, was introduced. Since the number of atoms along the distance is proportional to product

of the thickness and the density, the areal density, which represents the distances of the total mass of all atoms encountered by the radiation is a better unit when comparing the effectiveness of different shielding materials. [2]

3.4 Dosimetric units

Fluence Φ measures the number of particles dN incident on a sphere with cross section dA. Flux Ψ is the fluence measured during time interval dt.

$$d\Phi = \frac{dN}{dA} \tag{3.1}$$

$$d\Psi = \frac{d\Phi}{dt} \tag{3.2}$$

Fluence and flux are the clearest way of quantifying the radiation, and are used to evaluate the production and attenuation of secondary neutrons in this thesis.

Absorbed dose D is a basic dosimetirc unit, defined as the mean energy $d\bar{E}$ imparted into the target of mass dm by ionizing radiation, applicable to both direct and indirect ionizing radiation. The unit for absorbed dose is the Gray (Gy), where 1 Gray equals 1 joule per kilogram, $1Gy = 1J/kg$.

$$D = \frac{d\bar{E}}{dm} \tag{3.3}$$

Since radiation is frequently studied for its biological impact in both the space industry and the medical industry, dose equivalent is introduced to measure the exposure's impact on human body. The definition of dose equivalent is given by,

$$H = w_R \cdot D \tag{3.4}$$

where w_R is the dimensionless radiation weighting factor. Dose equivalent is measured in units of Sieverts (Sv), where 1 Sv is equal to 1 J/kg (joule/kilogram).

The radiation weighting factor w_R is determined by the type and energy of radiation. The larger the radiation weighting factor, means a bigger biological impact. Table 3.1 shows the weighting factors for different particles and energies recommended by ICRP 103 published in 2007. Most previous studies used weighting factors recommended by ICRP 60, where the weighting factors for protons are 5 and may be too conservative compared to the 1.5 recommended by NCRP 132. In ICRP 103, the radiation weighting factors for protons have been reduced from 5 to 2. [1] The radiation weighting factors for neutrons have been updated as well, from a step function to a continuous function of neutron energy. As shown in figure 3.2, the weighting factor for neutron is highly dependent on the neutron's energy. Neutrons of energy between $10^{-2} MeV$ to $10^3 MeV$ are relatively more harmful than the rest of the neutron energy spectrum.

Type of particle and energy	Radiation weighting factor w_R
Photons	1
Electrons and muons	1
Protons	2
α particles, fission fragments, heavy nuclei	20
Neutron	A continuous function of energy

Table 3.1 : Radiation weighting factor w_R for neutron recommended in ICRP 103 [1]

Dose equivalent results for different shielding materials have been simulated, with both ICRP 60 and ICRP 103, and the dose equivalent areal density curves have
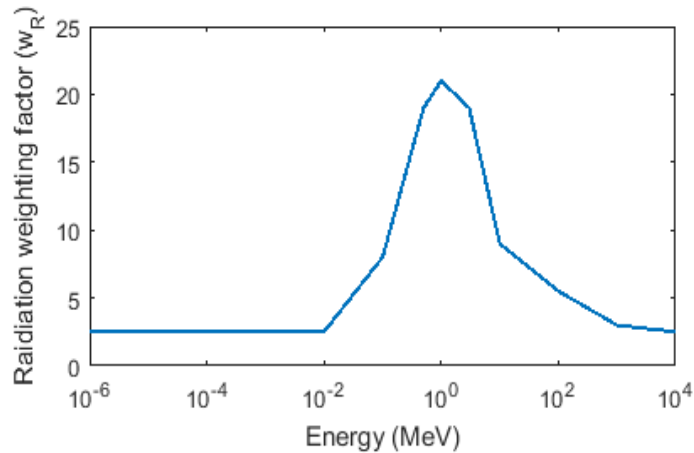
Figure 3.2 : Radiation weighting factors for neutron as a continuous function of neutron energy [1]

been plotted. Figure 3.3 shows that with the more recent weighting factors, the initial dose equivalent has dropped around 45%, as compared to that with ICRP 60. Furthermore, the total ionizing dose tends to drop faster with ICRP 103. This is because the primary and secondary protons have relatively larger flux and their flux drops more slowly than other ions. Since the weighting factors for protons decrease, the total dose equivalent changes accordingly.

In order to analyze the radiation effect on different tissues in the human body, effective dose E is defined as,

$$E = \sum_T w_T \sum_R w_R \cdot D_{T,R} \tag{3.5}$$

where $D_{T,R}$ is the absorbed dose deposited in tissue T by radiation R, w_T is the tissue weighting factor which ranges from 0.01 for skin tissue to 0.12 for bone marrow [13], and w_T for different tissues sum up to 1 for the whole human body.

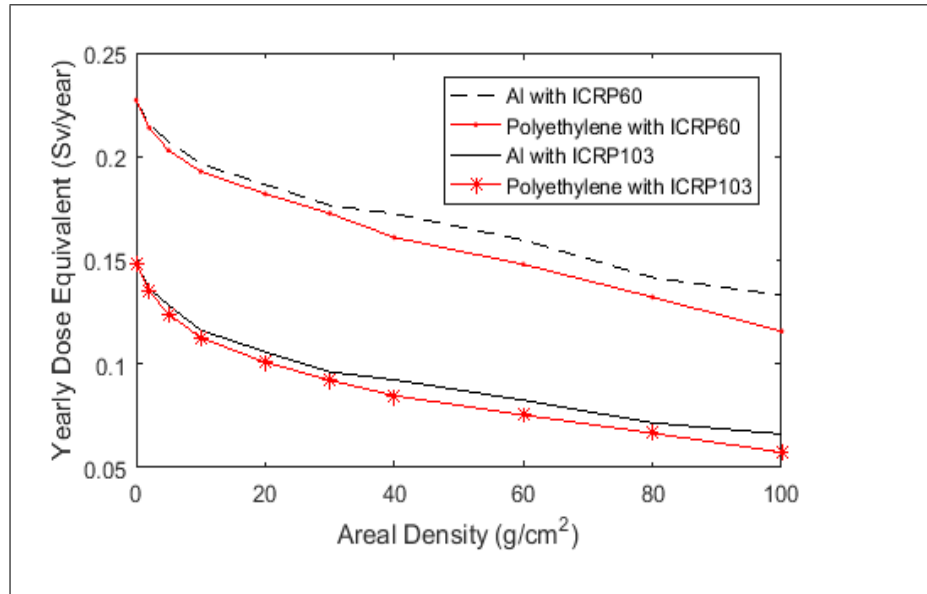Even yearly absorbed dose caused by GCR in shielding materials is relatively

Figure 3.3 : Yearly dose equivalent for different materials of varying areal density from 1977 Solar minimum GCR with weighting factor recommended by ICRP103

small, and thus so are their changes caused by varying areal density. This makes it hard to compare the shielding effectiveness of different materials. On the other hand, dose equivalent and effective dose, which consider relative contributions by different radiation species, show more noticeable differences as thickness increases. The dose equivalent analysis is presented in section 4.2.1 for single materials and in section 4.3 for multi-layer materials.

Fluence analysis has been rarely performed in former works. MULASSIS allows fluence analysis for electron, pion, muon, neutron, proton, and gamma. In fluence analysis, different particles are collected respectively. This makes fluence analysis very time consuming, but it is helpful in showing the detailed attenuation effect and fragmentation caused by different shielding and ions interactions. Fluence analysis is thus performed for secondary neutrons and presented in section 4.2.2.

Chapter 4

Radiation Shielding Strategy

4.1 Simulation setup

4.1.1 GCR model

The GCR model used as the input to MULASSIS is the CREME96 model during 1977 solar minimum in units of flux $(MeV^{-1}cm^{-2}s^{-1})$. Hydrogen, helium and iron ions are applied and assumed fully ionized. The GCR model is assumed to be isotropic and omnidirectional, which has been used as the angular distribution of GCR in MULASSIS.

4.1.2 Geometry

In this thesis, slabs made of different materials are used to represent shielding, as is shown in figure 4.1. The areal density of the total shielding ranges from 2 to $100g/cm^2$ in both dose equivalent analysis and fluence analysis.

Since the biological effect resulting from GCR is the major interest, it is important that proper material is used to model the human body. More than 70% of most organs are made of water, making water the best material for modeling the human body. Like in other studies [2] [8], a 30 g/cm^2 water phantom is used as the target in this thesis to collect the absorbed dose.
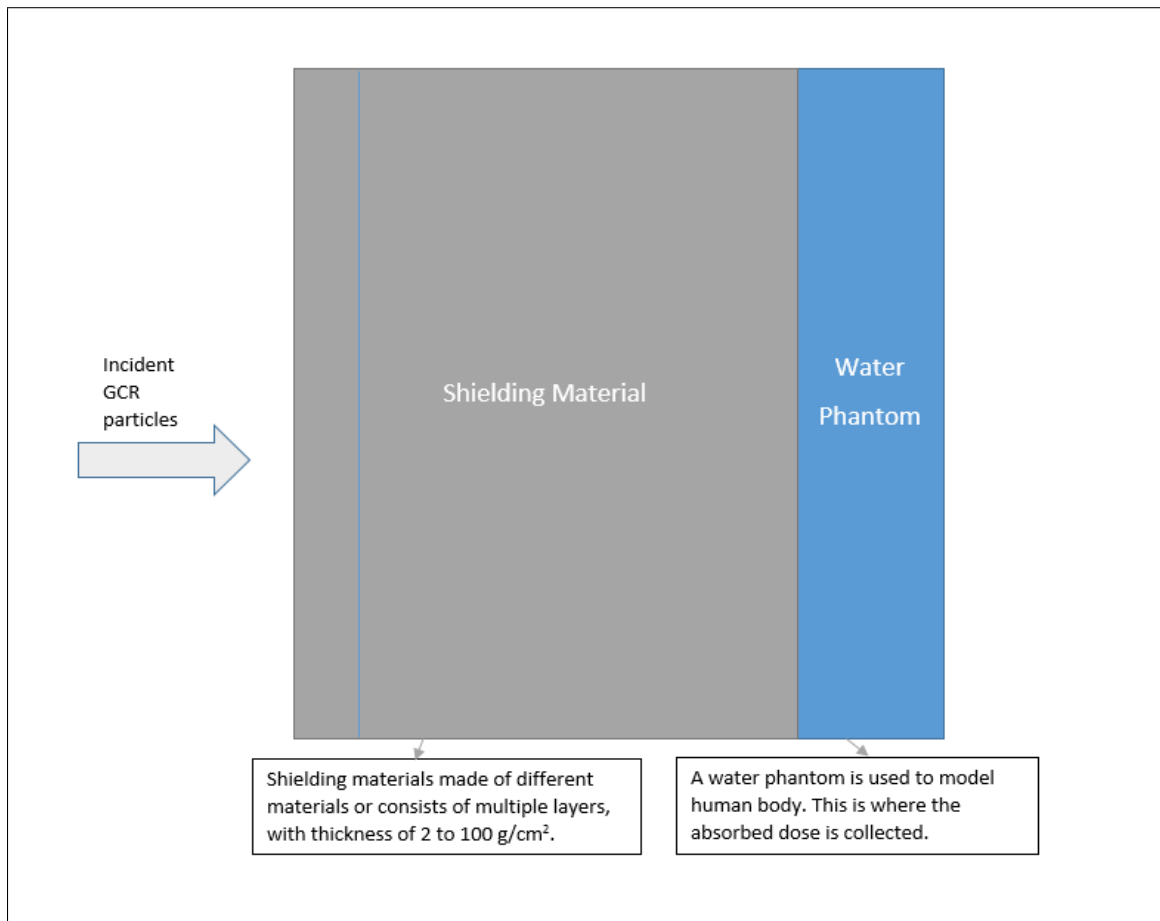
Figure 4.1 : Visualisation of geometry for dose analysis

4.1.3   Outputs and post-processing

The options for output units provided by MULASSIS include total ionizing dose in Gy, which is post-processed into dose equivalent in Sv by multiplying the radiation weighting factors. The dosimetric units are discussed in section 3.4. The dose-depth curves are plotted to show the shielding effect by different materials of varying areal density.

In order to examine the shielding effectiveness with respect to secondary effect, the fluence of neutrons are collected on the boundaries of the shielding materials of various areal densities, and analyzed for various neutron energies, and for GCR H, He, and Fe ions respectively.

4.1.4   Convergence study

A convergence study has been performed in order to examine the most appropriate number of primary particles to use in MULASSIS. As discussed in 2.3, the more primary particles used in a Monte Carlo code, generally the more accurate the results obtained. However, huge number of primary particles can make the simulation very time consuming. Thus, a convergence study has been performed in order to find an appropriate number that is both accurate and time-efficient.

MULASSIS offers primary particle numbers in powers of ten, from 10 to 10,000,000. Figure 4.2 shows the convergence study with three primary particle numbers, 10,000, 100,000, and 1,000,000. Results from using 100,000 and 1,000,000 agree well, meaning that the calculation converged at 100,000. Meanwhile 10,000 gives relatively inaccurate result, even though the simulations take shorter time to run. Therefore 100,000 was chosen as the the number of primary particle to use in later simulations with MULASSIS.
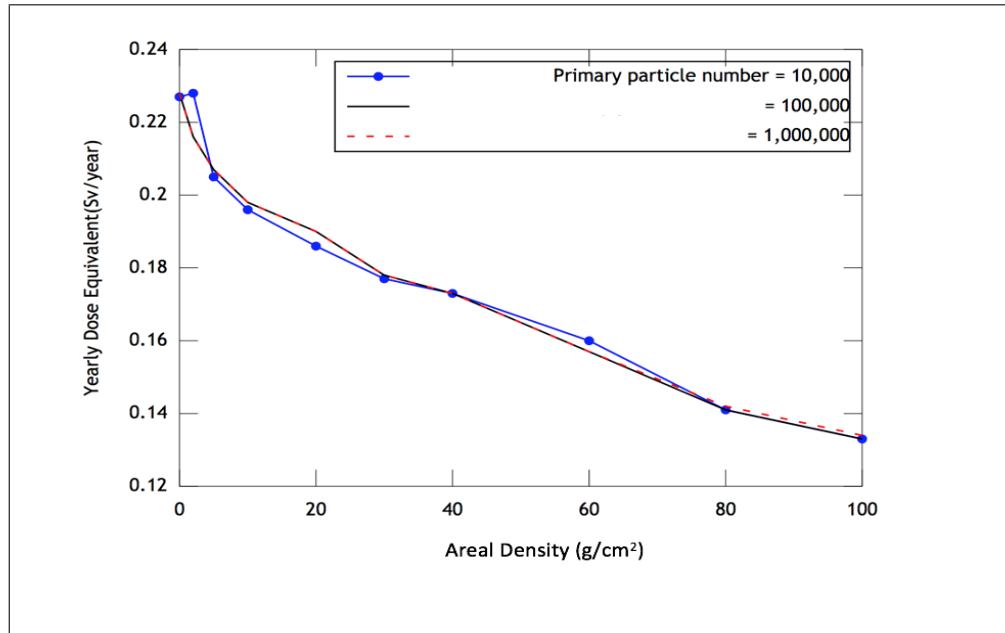
Figure 4.2 : Convergence study for MULASSIS performed with aluminum shielding from 0 to 100 g/cm^2 shielding against GCR

4.2 Shielding materials

Shielding from space radiation hazards has been a significant topic for decades. There are generally two categories for shielding, passive shielding and active shielding. Active shielding generates electromagnetic fields to deflect space radiation, which should have promising results, but is still under development. [3] Passive shielding takes advantage of the interactions between the radiation and the atoms in the shielding material to attenuate the radiation effect. A good passive shielding design should not only provides effectiveness in protection, but also be multifunctional, conformable with its application, cost-effective, nontoxic, durable and cause less secondary radiations. [14]

Since the Coulomb force is the dominate force in interactions between ions and

a shielding material, materials with the larger charge-to-mass ratio should be more effective. [2] On the contrary, heavy materials are not proper for shielding against GCR, because they can fragment during the interactions with these high energy ions.

The widely used passive shielding strategy for spacecraft is an aluminum layer of 5 g/cm^2, for its relatively low atomic number, light weight and structural stability. However, nuclear fission reactions take place when the GCR traverse aluminum walls and produce highly penetrating secondary fragments including neutrons and lighter ions.

Hydrogen, with the largest charge-to-mass ratio, is theoretically the most effective shielding material. Not only effective in slowing the GCR through direct ionization, hydrogen also has no neutrons, is the lightest element, and is effective in slowing secondary neutrons at the same time. Because the hydrogen nuclei have small mass, they cause more fragmentation of the HZE at first encounter. [9] Although hydrogen is not a structural material, its compounds with high hydrogen content, such as water, polyethylene, and lithium hydride, can be good candidates when applied with other structural materials like aluminum. In addition, hydrogen may have multiple uses, for example in alternative energy fuel cell applications.

With the thriving of nanoengineering, the proposed hydrogen storage in boron nitride nanotubes and carbon nanotubes can provide a material that is both structurally stable and shielding effective for radiation protection. Furthermore, boron has a high neutron cross section, making it a possible candidate in stopping the risky secondary neutrons. [14]

Given the discussion above, aluminum, polyethylene, boron nitride storing hydrogen and liquid hydrogen are selected herein as the materials of interest.

4.2.1   Dose equivalent analysis

The most effective shielding material in theory, liquid hydrogen, is first studied as a comparison with other materials. Aluminum is the current standard shielding material. Polyethylene is a representative for high hydrogen content material. Boron nitride infused with hydrogen is used to model the boron nitride nanotube storing hydrogen. These four materials are all studied in units of yearly dose equivalent and plotted for varying areal density.

The results given by MULASSIS are presented in figure 4.3, and are as anticipated. The curve that drops the fastest indicates the greater energy loss of the radiation, and thus the better shielding effectiveness. The curve for liquid hydrogen drops the fastest, followed by polyethylene and boron nitride plus hydrogen, while aluminum drops the slowest. Therefore, liquid hydrogen makes the most effective shielding material in theory. Polyethylene provides similar shielding effectiveness as Boron nitride infused with hydrogen. While both materials are more effective in shielding GCR than aluminum. So as between those two materials, the one with better structural stability might be the better shielding material.

4.2.2   Fluence analysis

As GCR ions travel into the shielding materials, inevitably neutrons are produced during nuclear fissions. In general, neutrons are the most harmful secondary radiation to the human body, especially with energy between $10^{-2} MeV$ to $10^3 MeV$. As in figure 3.2, the radiation weighting factor of neutrons can be more than 20. Fluence analysis is the most natural and clearest way to measure the radiation, and can help better decide which materials produce the less secondary neutrons, or which are the best at attenuating the secondary effect.
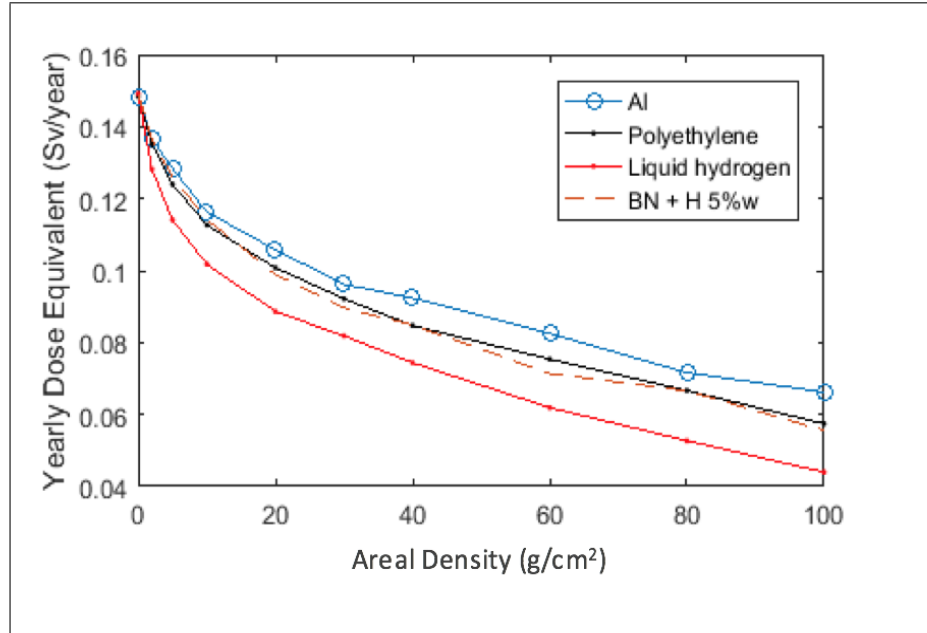
Figure 4.3 : Yearly dose equivalent for different materials of different areal densities against 1977 Solar minimum GCR with weighting factor recommended by ICRP 103

H, He and Fe ions in the GCR are input separately to aluminum, polyethylene, boron nitride, boron nitride plus hydrogen 5%w and liquid hydrogen. Then the consequent secondary neutron fluence are collected at the shielding boundaries and analyzed. Three dimensional graphs are plotted with the three axes being areal density of the shielding material (g/cm^2), the energy of the neutron (0 to 10^6 MeV) and the fluence ($particles/cm^2/(s)$) of neutrons respectively.

According to the plots in figure 4.4, with GCR protons incident on different materials, aluminum produces the most secondary neutrons. Compared to aluminum, polyethylene produces much less neutrons in total and in energy spectrum of 10^{-3} to 10^2 MeV. Boron nitride produces less neutrons than aluminum, but is still much worse than high hydrogen-content materials. Therefore boron nitride may not be a
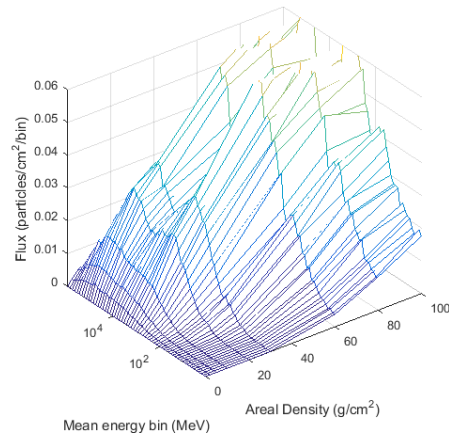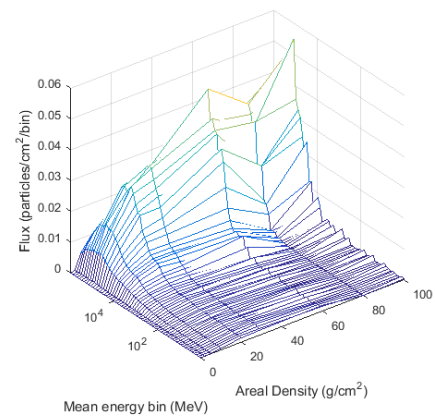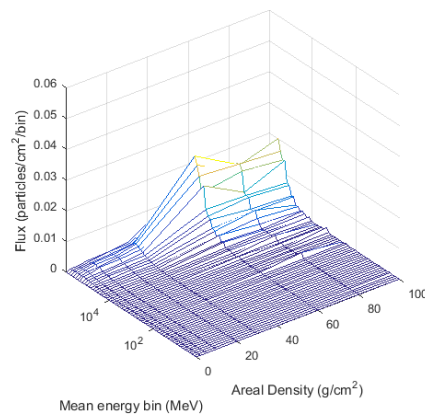
(a) Aluminum
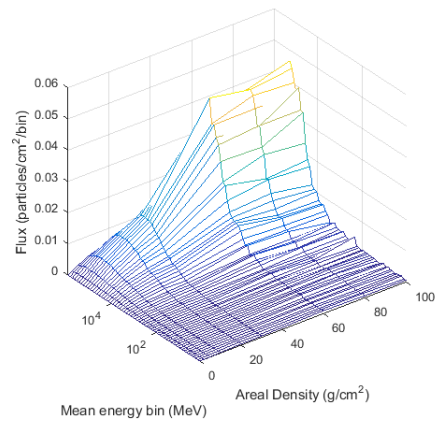
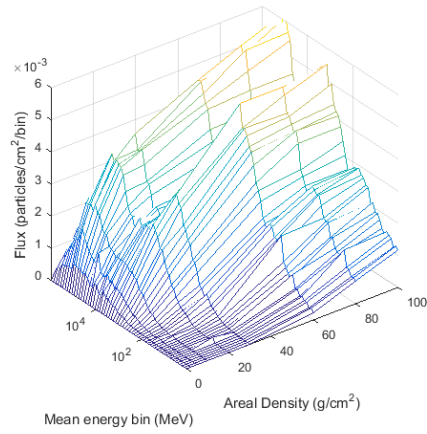(b) polyethylene
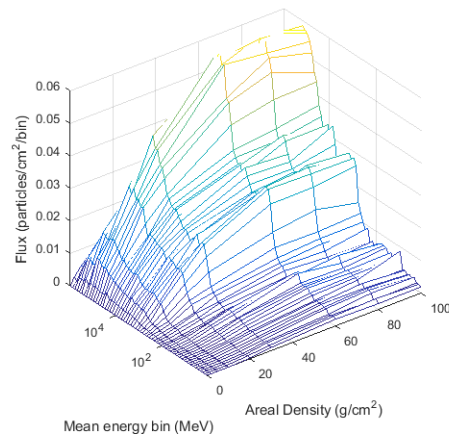
(c) Boron nitride
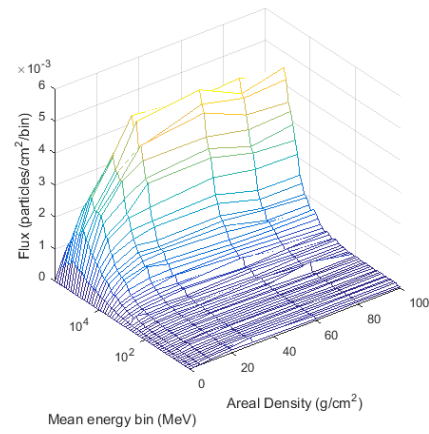
(d) Boron nitride + hydrogen 5%w
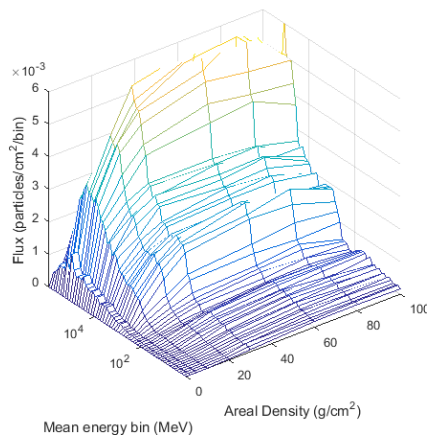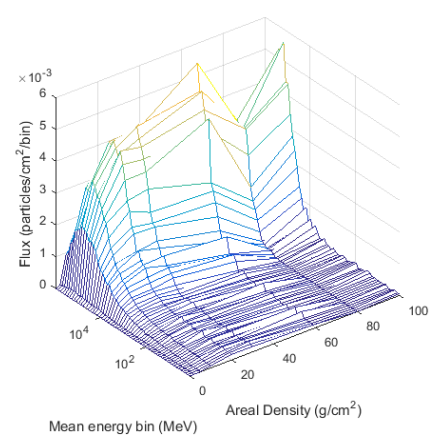

(e) Liquid hydrogen

Figure 4.4 : Secondary neutrons in shielding materials of varying areal density by GCR protons
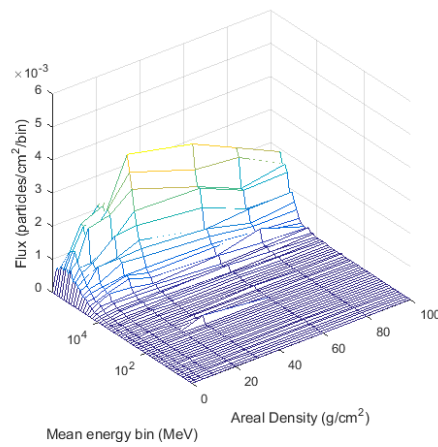
(a) Aluminum

(b) Polyethylene

(c) Boron nitride

(d) Boron nitride + hydrogen 5%w

(e) Liquid hydrogen

Figure 4.5 : Secondary neutrons in shielding materials of varying areal density by GCR He ions

(a) Aluminum

(b) Polyethylene
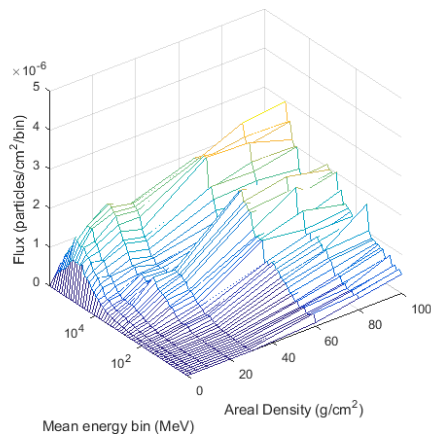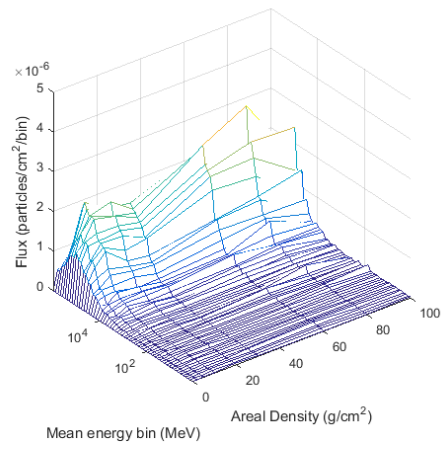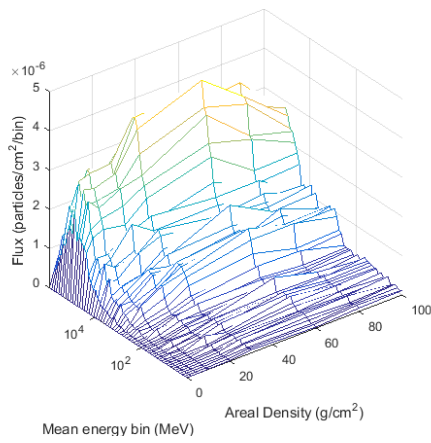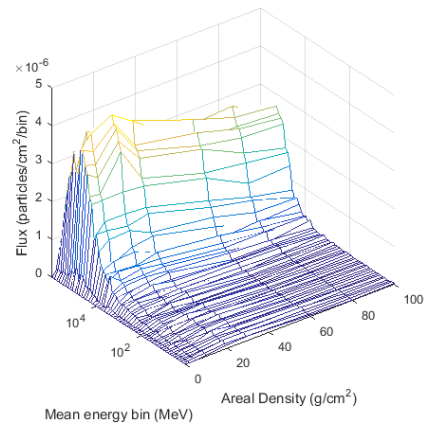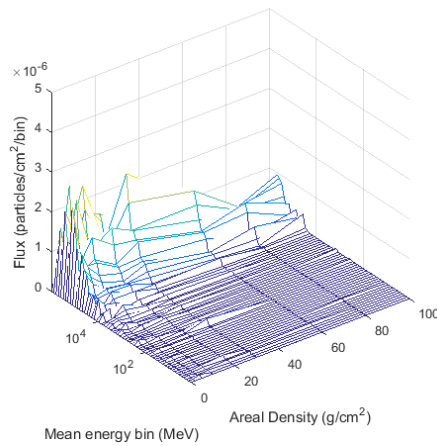
(c) Boron nitride

(d) Boron nitride + hydrogen 5%w

(e) Liquid hydrogen

Figure 4.6 : Secondary neutrons in shielding materials of varying areal density by GCR Fe ions

better shielding material than aluminum by itself. By adding the hydrogen content, the material produces less secondary neutrons in total and especially less in the most risky energy spectrum. Compared with the ideal liquid hydrogen shielding, polyethylene outperforms the other materials, followed by boron nitride plus 5% by weight hydrogen.

In terms of GCR He nuclei, the pattern of secondary neutron flux and energy is very similar to the results from GCR proton. As for Fe nuclei, boron nitride may be worse than aluminum, while polyethylene is still the best practical shielding material.

Hence, the current shielding material aluminum may not be effective in producing less secondaries. Higher hydrogen content can help attenuate the production of secondary neutrons. The future material, boron nitride nanotube storing hydrogen, with its structural stability and shielding effectiveness, may be a good candidate for effective shielding materials against GCR.

4.3   Multilayered shielding

In terms of being both effective shielding and multifunctional, combinations of materials can be a good solution, because each layer can address a particular radiation issue. As an example of multi-layered shielding, graded Z shielding has already been studied in protection for electronics in the trapped electron belt, where many satellites operate.

In terms of multilayered shielding for GCR, a combination of aluminum and polyethylene slabs is currently being used by NASA in International Space Station (ISS). [3] The multilayered shielding of Al2024 alloy and polyethylene structure has been studied with HZETRN [4], and results show that the dual layer has a much better shielding effectiveness than a single aluminum layer of the same areal density
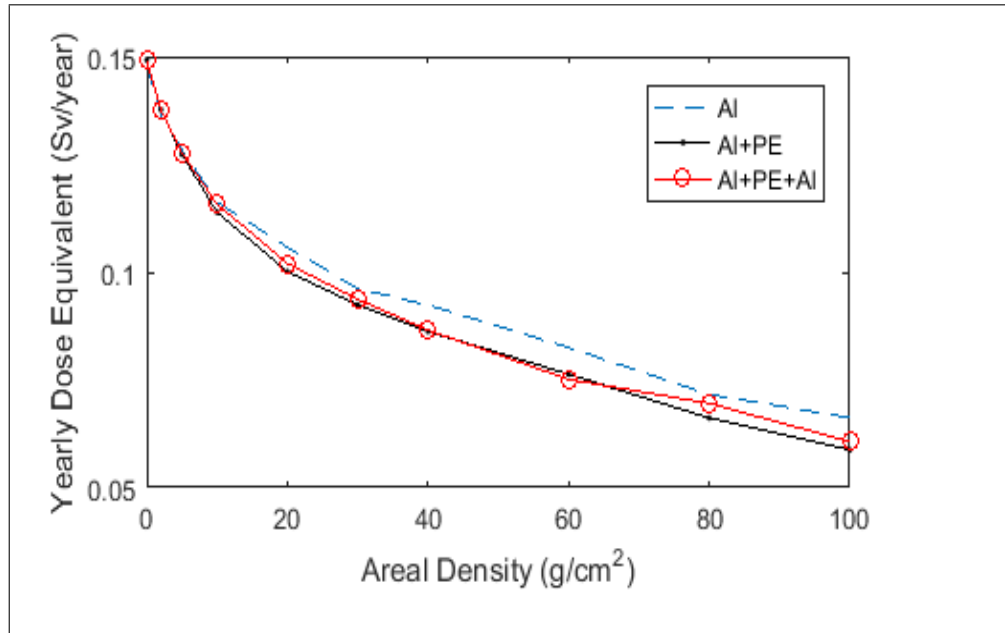
Figure 4.7 : Yearly dose equivalent for multilayered shielding against 1977 Solar minimum GCR with PE as dominating shielding

(g/cm^2).

In this thesis, the shielding effectiveness of two combinations of aluminum and polyethylene are studied. The first combination is aluminum of 2 g/cm^2 and polyethylene of $0 - 98g/cm^2$. The second combination is a "sandwich" Al-PE-Al structure proposed in [4]. These two kinds of Al-PE multilayers are studied with MULASSIS and compared to shielding of aluminum alone, the results of which are shown in figure 4.7. By adding the polyethylene layer, the shielding effectiveness is improved by 6%.

In order to compare the shielding ability against GCR secondary neutron, polyethylene and boron nitride plus hydrogen of 5% by weight are then selected as the second layer of the shielding respectively. The results are shown in fig 4.8. As anticipated, the shielding effectiveness of Al- BN+H structure is similar and better than that of
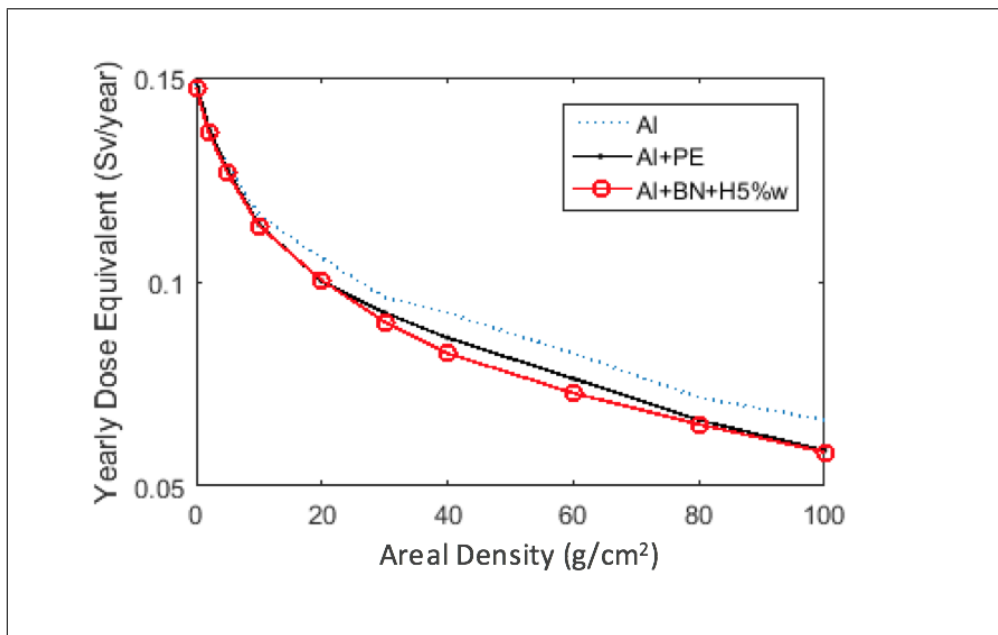
Figure 4.8 : Yearly dose equivalent for multilayered shielding against 1977 Solar minimum GCR with boron nitride+ hydrogen 5% by weight compared with polyethylene dominated shielding

Al-PE at the same areal densities. This is most likely because of the high effectiveness by H content and the high neutron cross section of boron.

Chapter 5

Conclusions

The space radiation is extremely biologically damaging. This is one of the biggest obstacles for the future missions into deeper space. Therefore, more effective shielding materials are demanded. Shielding materials can be studied with radiation transport codes, which include deterministic codes and Monte Carlo codes. MULASSIS is a Monte Carlo code developed based on Geant4 and is used for simulations in this thesis.

Among the natural sources of space radiation, the Galactic Cosmic Rays are composed of fully ionized particles travelling at near relativistic speeds from outside the solar system. With extremely high energy and high charge, these ions are especially hard to shield. Furthermore, as they penetrate the external environment, even more dangerous secondary particles are produced.

CREME96 during 1977 solar minimum has been used as input to MULASSIS. Slabs of 0 to 100 g/cm^2 have been used to model shielding materials. A water phantom of 30 g/cm^2 has been used to model the target– human body.

In order to choose more suitable shielding materials against GCR, the physical interactions of ionizing radiation is discussed. High hydrogen-content materials should be more effective in shielding against GCR. Boron nitride, with a high neutron cross section, could also be a good candidate in stopping secondary neutrons. Therefore, dose equivalent and fluence analyses have been performed for aluminum, polyethylene, boron nitride infused with hydrogen and liquid hydrogen to study the energy

deposition and production of secondary neutrons.

According to the dose equivalent analyses, both polyethylene and boron nitride plus hydrogen are more effective than aluminum, but still worse than liquid hydrogen, which is the most effective shielding material in theory. By increasing the hydrogen content, the production of the dangerous secondary neutrons decreases noticeably. With the structural advantages, boron nitride nanotubes storing hydrogen may be a potentially effective shielding material against GCR.

In future studies, dose analyses calculation can be done with deterministic code and compared with the Monte Carlo results. More GCR ions should be considered for a more thorough study of the shielding effect. Moreover, better modelling of the molecular structure of boron nitride storing hydrogen can be applied to obtain more accurate results.

Bibliography

[1] J. Valentin *et al.*, *The 2007 recommendations of the international commission on radiological protection.* Elsevier Oxford, UK, 2007.

[2] J. Wilson, J. Miller, A. Konradi, and F. Cucinotta, "Shielding strategies for human space exploration," 1997.

[3] M. Durante, "Space radiation protection: destination mars," *Life sciences in space research*, vol. 1, pp. 2–9, 2014.

[4] A. Borggräfe, M. Quatmann, and D. Nölke, "Radiation protective structures on the base of a case study for a manned mars mission," *Acta Astronautica*, vol. 65, no. 9, pp. 1292–1305, 2009.

[5] F. Lei, R. Truscott, C. Dyer, B. Quaghebeur, D. Heynderickx, R. Nieminen, H. Evans, and E. Daly, "Mulassis: A geant4-based multilayered shielding simulation tool," *IEEE Transactions on Nuclear Science*, vol. 49, no. 6, pp. 2788–2793, 2002.

[6] G. Santin, "Chapter ii radiation interaction physics and simulation,"

[7] S. Agostinelli, J. Allison, K. a. Amako, J. Apostolakis, H. Araujo, P. Arce, M. Asai, D. Axen, S. Banerjee, G. Barrand, *et al.*, "Geant4a simulation toolkit," *Nuclear instruments and methods in physics research section A: Accelerators,*

Spectrometers, Detectors and Associated Equipment, vol. 506, no. 3, pp. 250–303, 2003.

[8] J. Bernabeu and I. Casanova, "Geant4-based radiation hazard assessment for human exploration missions," *Advances in Space Research*, vol. 40, no. 9, pp. 1368–1380, 2010.

[9] J. Adams Jr, D. Hathaway, R. Grugel, J. Watts, T. Parnell, J. Gregory, and R. Winglee, "Revolutionary concepts of radiation shielding for human exploration of space," 2005.

[10] S. S. Board, N. R. Council, *et al.*, *Space radiation hazards and the vision for space exploration: report of a workshop.* National Academies Press, 2006.

[11] A. J. Tylka, J. H. Adams, P. R. Boberg, B. Brownstein, W. F. Dietrich, E. O. Flueckiger, E. L. Petersen, M. A. Shea, D. F. Smart, and E. C. Smith, "Creme96: A revision of the cosmic ray effects on micro-electronics code," *IEEE Transactions on Nuclear Science*, vol. 44, no. 6, pp. 2150–2160, 1997.

[12] "Course note of mech592 by dr. leory chiao, mechanical engineering, rice university,"

[13] A. D. Wrixon, "New icrp recommendations," *Journal of Radiological Protection*, vol. 28, no. 2, p. 161, 2008.

[14] S. A. Thibeault, J. H. Kang, G. Sauti, C. Park, C. C. Fay, and G. C. King, "Nanomaterials for radiation shielding," *MRS Bulletin*, vol. 40, no. 10, pp. 836–841, 2015.